

Direct observation of the enhanced photonic spin Hall effect in a subwavelength grating

N. I. Petrov^{1}, Y. M. Sokolov¹, V. V. Stoiakin¹, V. A. Danilov¹, V. V. Popov², and B. A. Usievich²*

¹Scientific and Technological Centre of Unique Instrumentation of the Russian Academy of Sciences, Moscow, Russia

²Lomonosov Moscow State University, Moscow, Russia

*Corresponding author: petrovni@mail.ru

KEYWORDS: photonic spin Hall effect, surface plasmon resonance, subwavelength grating, degree of polarization, spin separation purity

ABSTRACT. The photonic spin Hall effect (PSHE) in surface plasmon resonance (SPR) structures has great potential for various polarization-sensitive applications and devices. Here, using optical weak measurement, we observe spin-dependent and spin-independent angular shifts of the reflected beam, enhanced by SPR in a subwavelength nickel grating. An enhanced in-plane photonic spin Hall effect manifested in the angular splitting of circularly polarized photons with opposite helicity signs is demonstrated. We theoretically and experimentally demonstrate that angular in-plane shifts can be changed from spin-independent (Goos-Hanchen shift) to spin-dependent (PSHE) when the incident beam polarization state changes. The SPR-induced depolarization of light and the mixing of polarization states are analyzed. High purity of spin

separation and a high degree of circular polarization are achieved with an optimal polarization state (preselection angle) and a resonance angle of incidence. The spineless spatial separation of two orthogonal components of the field with diagonal linear polarizations is demonstrated.

A light beam being reflected or refracted at the interface, experiences spatial and angular shifts depending on its polarization and intensity profile. Both reflected and refracted beams are formed as a result of interference of waves reradiated in neighboring media. The analysis revealed many interesting phenomena, including the well-known spin-independent Goos-Hanchen (GH) and spin-dependent Imbert-Fedorov (IF) shifts in the plane and out-of-plane of propagation of the incident beam, respectively [1-4]. A significant increase in the GH shift is achieved by excitation of surface plasmon waves [5-8] and Bloch surface electromagnetic waves in photonic crystals [9]. A noticeable increase in the angular displacement can be observed for a tightly focused beam reflected by a dielectric surface near the Brewster angle [10]. The physical origin of the lateral GH shift lies in the angular dispersion of the Fresnel reflection coefficients. The IF shift is a spin-dependent effect that occurs as a result of spin-orbit interaction [4]. In the last decade, the spin Hall effect of light (SHEL) has been intensively studied in various physical systems [11-28].

Usually, PSHE as well as IF shift is associated with the spatial and angular separation of photons with opposite spin angular momentum (SAM). Spin-dependent transverse shifts between the left and right circularly polarized components were observed for photons passing through the air-glass interface [14-16]. Subsequently, the longitudinal (in-plane) photonic spin splitting was observed [17-21]. In particular, the IF shift of $3.2 \mu\text{m}$ was observed for the light incident on the surface near the Brewster angle [16]. The large transverse SHEL effect was demonstrated for a

beam passing through a tilted polarizer [22, 23]. In [24], an enhanced optical spin Hall effect was demonstrated in a thin vertical hyperbolic metamaterial. A 0.16 mm displacement of separated reflected light spots corresponding to opposite circular polarizations was observed in a planar waveguide via ultrahigh-order modes [26]. A significant enhancement of the SHEL effect occurs via the surface plasmon resonance (SPR) [27, 28]. Although PSHE has been well studied to date, there is still no effective way to control the spin angular shift, especially to increase its magnitude or switch the spatial position of the reflected beam.

In this paper, we demonstrate the spin Hall effect of light in the light reflection from a subwavelength nickel grating enhanced by SPR. Using the standard SHEL theory, we show that in-plane angular shifts can be changed from spin-independent (Goos-Hanchen shift) to spin-dependent (PSHE) when the polarization state of the incident beam slightly changes. We verify our simulations experimentally using the polarimetric and quantum weak measurement methods. SPR induced depolarization of light and mixing of polarization states are analyzed. A novel phenomenon of the spin-independent splitting of two orthogonal field components with linear polarizations is described.

In Figure 1a the experimental setup consisting of a He-Ne laser, half-wave and quarter-wave plates, a linear polarizer, a focusing lens, a subwavelength diffraction grating, and a CCD camera for measuring the beam profile is presented. The angular resolution of the motorized rotating platform on which the diffraction grating is mounted is 0.0005° . The angle measurement error (repeatability) is $0.005^\circ=18''$. Figure 1b illustrates the reflection of the beam from the air-grating interface. The coordinate frames (x_i, y_i, z_i) and (x_r, y_r, z_r) correspond to the incident and reflected electric fields.

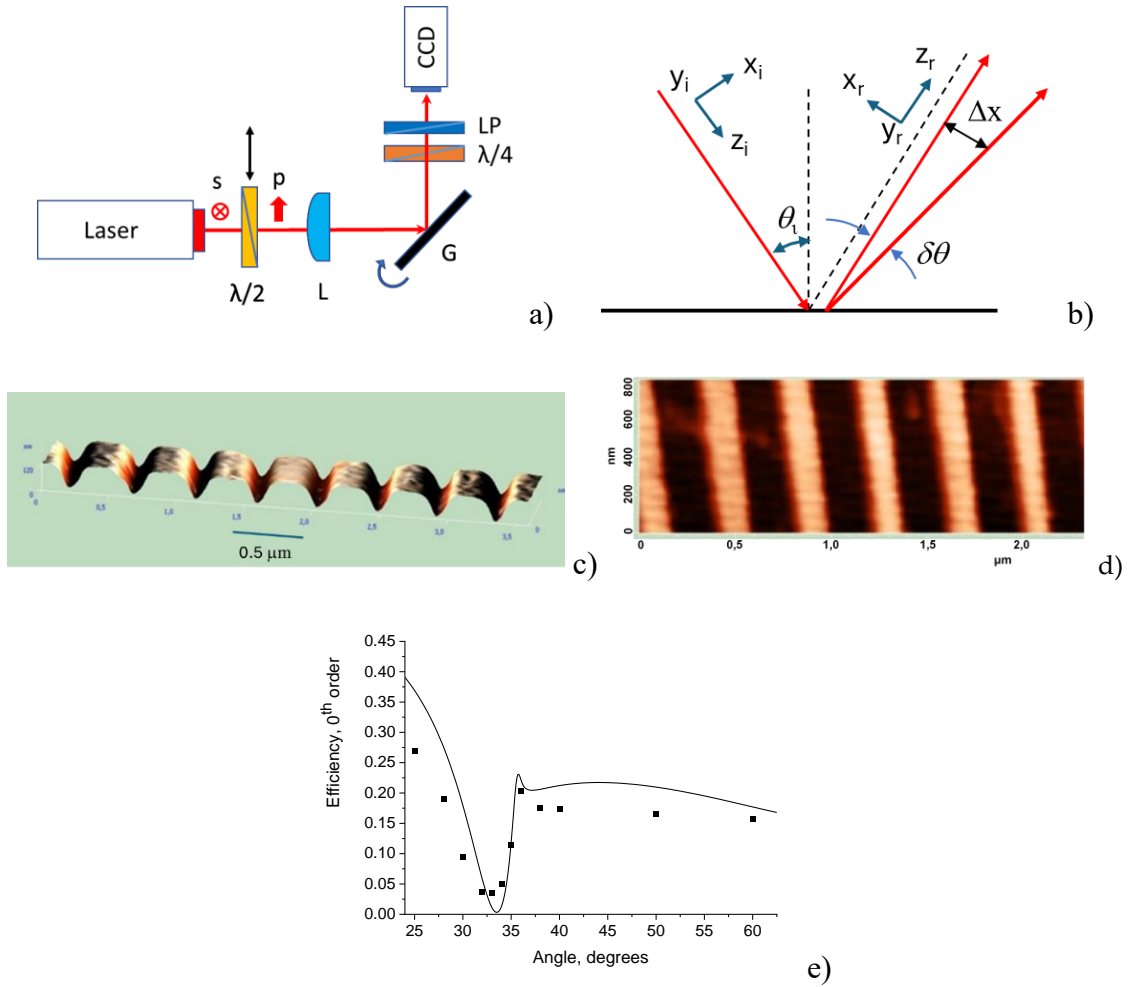


Figure 1. (a) Experimental setup. $\lambda/2$ – half-wave plate, L – lens, G – subwavelength grating, $\lambda/4$ – quarter-wave plate, LP – linear polarizer, and CCD – camera. (b) Schematic diagram of the in-plane PSHE when the beam is reflected from the grating surface. (c, d) AFM image of a subwavelength grating with a period $\Lambda = 400$ nm and (e) calculated and measured diffraction efficiency of zero-order depending on the angle of incidence for a nickel grating with a period of $\Lambda = 400$ nm and a depth of $h = 80$ nm at a wavelength of radiation $\lambda = 632.8$ nm with p -polarization.

We investigate angular shifts when the surface plasmon resonance is excited in a subwavelength nickel grating with a period of $\Lambda = 400$ nm and a depth of $h = 80$ nm (Figure 1c,

d). Note that the angular shift is easier to measure because of an additional enhancement caused by the propagation factor. The effects of angular shift and beam shape change for a reflected beam near surface plasmon resonance conditions are demonstrated experimentally and confirmed by rigorous electromagnetic simulations. Optimal conditions for the coupling of incident light with a surface plasmon wave is achieved at a grating depth of $h = 80$ nm and a resonant angle of incidence of $\theta_i = 33.53^\circ$ (Figure 1e). A significant increase in the angular shift with a decrease in the incident beam width is shown.

A rigorous electromagnetic theory based on the C - method is used for the calculations [6, 7]. Note that an s - wave does not excite surface plasmon waves, so a p - polarized incident wave is necessary to observe the surface plasmon resonance.

The electric field of the reflected beam can be described using the standard SHEL theory [4, 13, 16]. The complex amplitude of the reflected beam can be expressed as Fourier transformation:

$$\mathbf{E}(x_r, y_r, z_r) = \iint \mathbf{E}(k_{rx}, k_{ry}, z_r) e^{ik_{rx}x + ik_{ry}y} dk_{rx} dk_{ry}, \quad (1)$$

where the angular spectrum in the paraxial approximation is given by

$$\mathbf{E}(k_{rx}, k_{ry}, z_r) = \mathbf{E}_0(k_{rx}, k_{ry}) e^{iz_r \sqrt{k_0^2 - k_{rx}^2 - k_{ry}^2}} \cong \mathbf{E}_0(k_{rx}, k_{ry}) e^{ik_0 z_r} e^{-\frac{i}{2k_0}(k_{rx}^2 + k_{ry}^2)z_r}, \quad (2)$$

where $k_0 = 2\pi/\lambda$ is the incident wave vector, and k_{rx}, k_{ry} are the components of the wave-vector of the reflected beam in x_r, y_r direction.

Based on the boundary condition, the reflected angular spectrum is expressed as [13, 16]:

$$\begin{bmatrix} E_r^p \\ E_r^s \end{bmatrix} = \begin{pmatrix} r_p & \frac{k_{ry}(r_p + r_s) \cot \theta_i}{k_0} \\ -\frac{k_{ry}(r_p + r_s) \cot \theta_i}{k_0} & r_s \end{pmatrix} \begin{bmatrix} E_i^p \\ E_i^s \end{bmatrix}, \quad (3)$$

where r_p and r_s are the Fresnel reflection coefficients for p - and s - polarizations, respectively, θ_i is the incident angle, $k_{rx} = -k_{ix}$, and $k_{ry} = k_{iy}$.

Decomposing into a Taylor series in the vicinity of the central wave vector $k_{ix0} = k_0 \sin \theta_0$, r_p and r_s can be represented as:

$$r_{p,s}(\theta_i) = r_{p,s}(\theta_0) + (\theta_i - \theta_0) \left[\frac{dr_{p,s}}{d\theta_i} \right]_{\theta_i=\theta_0} + \dots \quad (4)$$

Consider the incident p - polarized beam with a Gaussian angular spectrum:

$$E_i^p = \frac{w_0}{\sqrt{2\pi}} \exp \left[-\frac{w_0^2 (k_{ix}^2 + k_{iy}^2)}{4} \right], \quad (5)$$

where w_0 is the beam waist.

Calculating the integral in Eq. (1) using Eqs. (3) - (5) and relationships $E_r^p = \frac{1}{\sqrt{2}} (E_r^+ + E_r^-)$

and $E_r^s = \frac{i}{\sqrt{2}} (E_r^- - E_r^+)$, we obtain the expression for the right- and left- handed circularly polarized components of the reflected field

$$E_r^\pm = \frac{1}{\sqrt{2\pi w_0}} \frac{z_R}{z_R + iz_r} \exp \left(-\frac{k_0}{2} \frac{x_r^2 + y_r^2}{z_R + iz_r} \right) \left[r_{p,s} - \frac{ix_r}{z_R + iz_r} \frac{dr_{p,s}}{d\theta_i} \mp \frac{y_r \cot \theta_i}{z_R + iz_r} (r_p + r_s) \right], \quad (6)$$

where the positive and negative signs denote the right circularly polarized (RCP) and the left circularly polarized (LCP) field components, and $z_R = k_0 w_0^2 / 2$ is the Rayleigh length.

In Figure 2, the measured and calculated intensity profiles of left- handed circularly polarized component of the reflected beams passing through a CPL filter, which includes a quarter-wave plate and a linear polarizer, are presented at a distance of $z = 25$ cm from the grating surface for different angles of incidence. An incident Gaussian beam with a beam waist $w_0 = 22.6 \mu\text{m}$ is p - polarized. It follows from this that in-plane spin-independent beam splitting (without separation of photons with opposite SAM), which is the GH shift, occurs for an incident p - polarized beam. The appearance of two spots around the resonant angle of incidence is due to the presence of a

dip in the reflectivity curve (Figure 1e). It is seen from Figures 2a and 2c, that the deviation of the angle of incidence in one direction or another from the resonant angle leads to a change in the spatial position of the reflected beam.

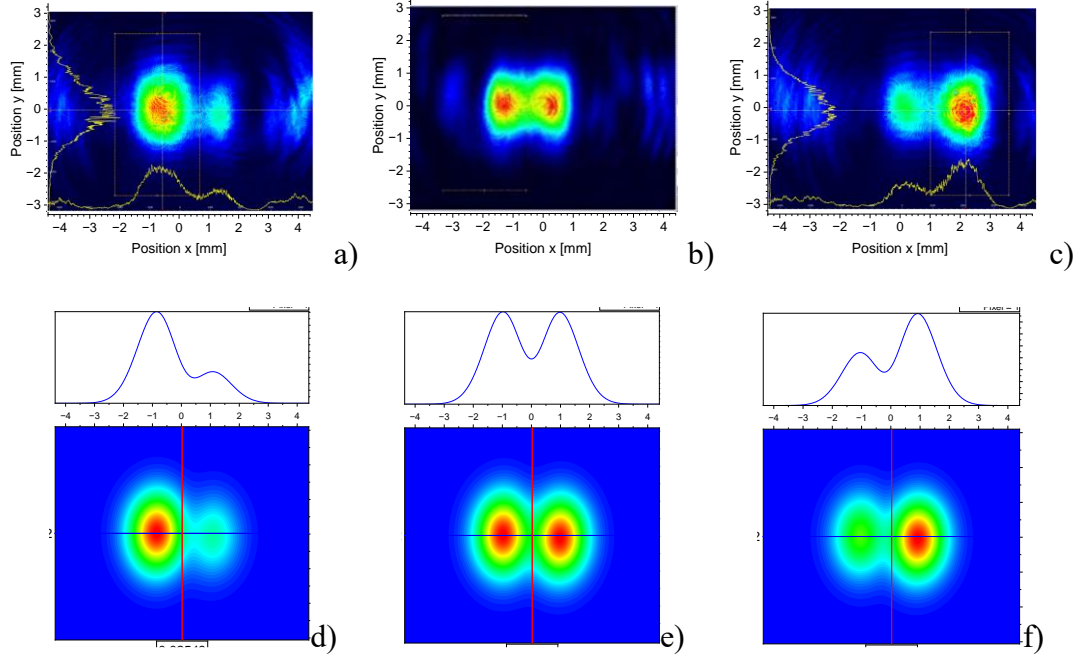


Figure 2. Measured (a, b, c) and calculated (d, e, f) intensity profiles of reflected beams passing through the CPL filter. (a, d) $\theta_i = 33.48^\circ$, (b, e) $\theta_i = 33.53^\circ$, (c, f) $\theta_i = 33.58^\circ$.

To observe the enhanced in-plane spin-dependent splitting an optimal overlap of the preselection and post-selection states should be created. This makes it possible to observe the enhancement of spin Hall shift by controlling the polarization of the incident beam. In this case, the incident beam becomes elliptically polarized (contains p - and s - polarization components) and the reflected beam is expressed as:

$$\begin{bmatrix} E_{rw}^p \\ E_{rw}^s \end{bmatrix} = \begin{bmatrix} r_p \cos \gamma + \frac{k_{ry}(r_p + r_s) \cot \theta_i \sin \gamma}{k_0} \\ r_s \sin \gamma - \frac{k_{ry}(r_p + r_s) \cot \theta_i \cos \gamma}{k_0} \end{bmatrix} \tilde{E}_i(k_{ix}, k_{iy}), \quad (7)$$

where γ is the linear polarization angle of incident beam (preselection angle) between the polarization vector and horizontal axis x_i , and $\tilde{E}_i = \frac{w_0}{\sqrt{2\pi}} \exp\left[-\frac{w_0^2(k_{ix}^2 + k_{iy}^2)}{4}\right]$.

For this preselection, the in-plane spin splitting undergoes significant amplification. It follows from Eq. (7) that the center of gravity (centroid position) of the circularly polarized component of the reflected beam is expressed as

$$\langle x^\pm \rangle = \frac{\langle E^\pm | x | E^\pm \rangle}{\langle E^\pm | E^\pm \rangle} = \frac{2\sqrt{z_R^2 + z_r^2} |\dot{r}_p| \cos\gamma (a_p \cos\gamma \mp a_s \sin\gamma)}{2k_0 z_R (a \pm b) + |\dot{r}_p|^2 \cos^2\gamma}, \quad (8)$$

where E^\pm are the electric fields that are right- and left- handed circularly polarized, respectively, $a_p = -|r_p| \sin(\varphi_p + \gamma_1 - \gamma_2)$; $a_s = |r_s| \cos(\varphi_s + \gamma_1 - \gamma_2)$; $a = |r_p|^2 \cos^2\gamma + |r_s|^2 \sin^2\gamma$; $b = |r_p| |r_s| \sin(2\gamma) \sin(\varphi_p - \varphi_s)$, $z_R + iz_r = \sqrt{z_R^2 + z_r^2} e^{i\gamma_1}$, $z_R = k_0 w_0^2 / 2$, $r_p = |r_p| e^{i\varphi_p}$, $r_s = |r_s| e^{i\varphi_s}$, $\dot{r}_p = |\dot{r}_p| e^{i\gamma_2}$, $\dot{r}_p = \frac{\partial r_p}{\partial \theta_i}$.

At the optimal preselection angle, we clearly observe the in-plane angular splitting of reflected light with opposite circular polarizations. The optimal preselection angle corresponds to the condition under which the amplitude of reflected light with p - polarization becomes equal to the amplitude of reflected light with s -polarization.

In Figure 3, the in-plane spin splitting for the preselection angle $\gamma = 4^\circ$ is shown. When the reflected beam passes through a filter of a certain circular polarization, one of the spots disappears. This means that there is a spatial separation of left-handed and right-handed circularly polarized photons. The physical mechanism of such separation is related to the spin-orbit interaction enhanced by surface plasmon resonance in a subwavelength diffraction grating.

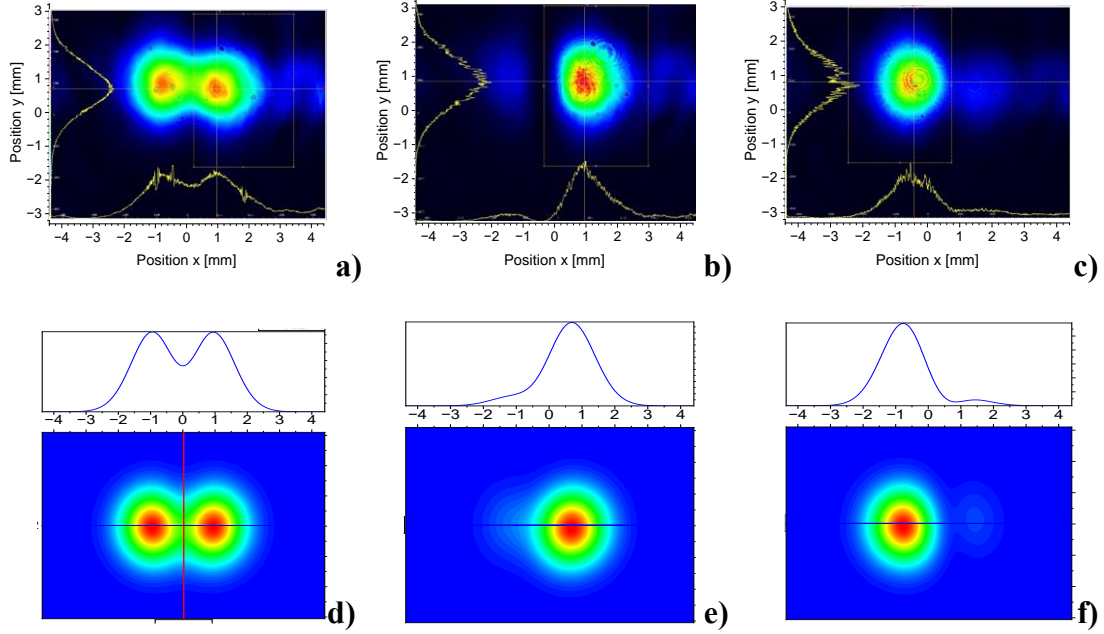


Figure 3. Measured (a, b, c) and calculated (d, e, f) intensity profiles of the reflected beams at a distance of $z = 25$ cm from the grating surface. $\theta_i = \theta_{res} = 33.53^\circ, \gamma = 4^\circ$. (a, d) without polarizers, (b, e) after passing the CPL filter, and (e, f) after passing the CPR filter.

The LCP and RCP (left-handed and right-handed circularly polarized) components of the reflected beam are well separated along the x axis, i.e., they are shifted in opposite directions. The left and right spots have circular polarizations with opposite signs of helicity. Photons with a given helicity are shifted in the opposite direction when the preselection angle changes its sign.

In Figure 4, the influence of the preselection angle on the position of the reflected beam with circular polarization is shown. When choosing the optimal preselection angle, a high degree of spin separation is achieved. In Figures 4g and 4h, the dependences of the position of the intensity peak x_m and the position of the center of gravity $\langle x_- \rangle$ on the preselection angle are presented. The centroid position of the reflected beam is given by Eq (8).

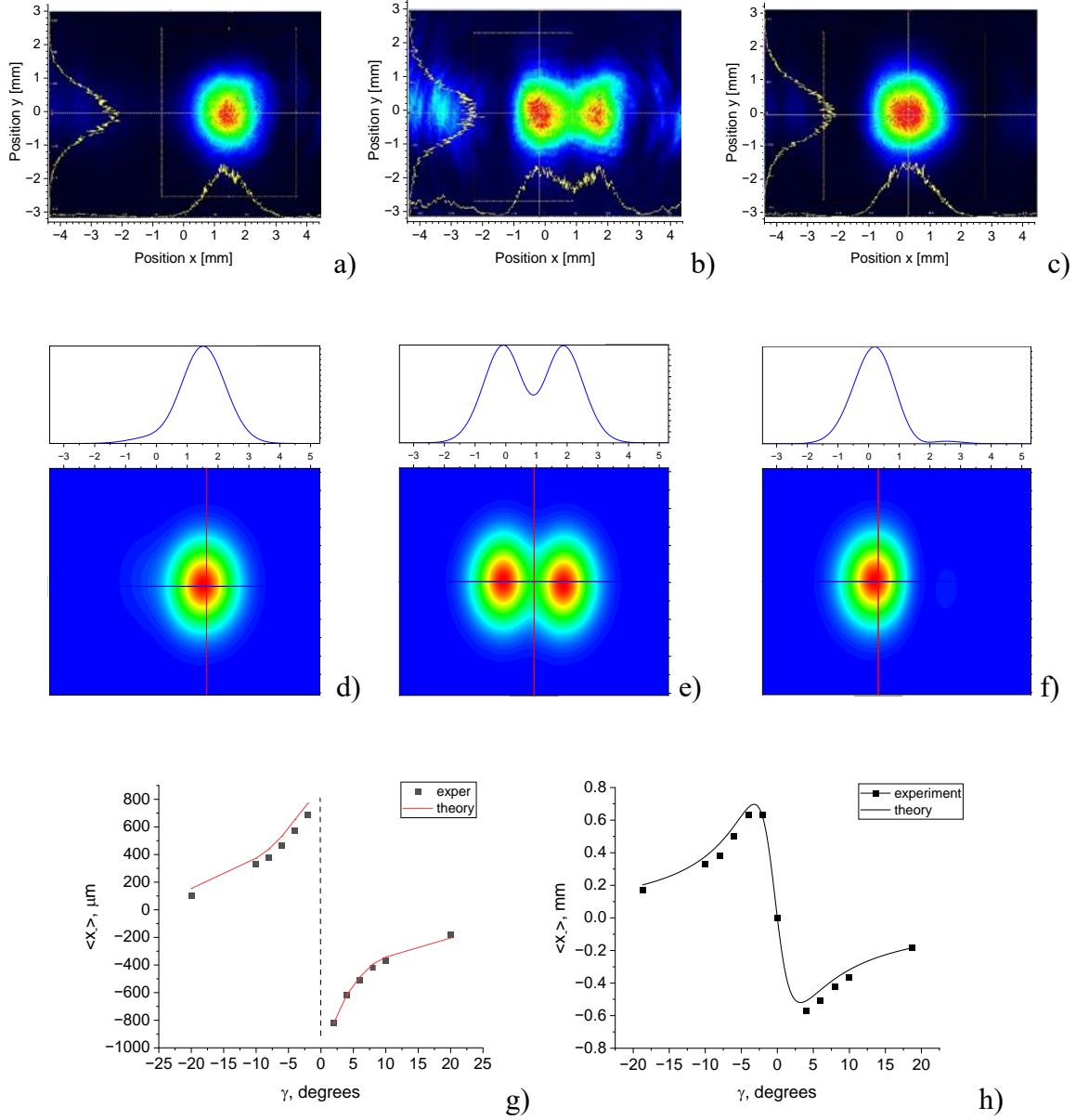


Figure 4. Measured (a, b, c) and calculated (d, e, f) intensity profiles of reflected beams passing through the CPL filter at a distance of $z = 25$ cm from the grating surface. $\theta_i = \theta_{res} = 33.53^\circ$, (a, d) $\gamma = -4^\circ$, (b, e) $\gamma = 0^\circ$, and (c, f) $\gamma = 4^\circ$. Angular shifts of the peak intensity position (g) and the centroid position (h) of the reflected beam as function of the preselection angle γ .

It can be seen that there is no SHE at the preselection angle $\gamma = 0$ (Figures 4b and 4e). However, the apparent spin splitting occurs at a nonzero preselection angle reaching the maximum separation distance between beams with opposite circular polarization at $\gamma = \pm 4^\circ$ (Figures 4a and 4c). The measurements show that the positions of the intensity peaks and centroids are in good agreement with the simulation results.

It follows from the measurements that reflected light under SPR conditions is depolarized and polarization states are mixed because of the interaction of incident light with surface plasmon-polariton waves.

The degree of polarization (DOP) is defined as

$$P = (\eta_1^2 + \eta_2^2 + \eta_3^2)^{1/2}, \quad (9)$$

where $\eta_1 = \frac{I(0)-I(90)}{I(0)+I(90)}$, $\eta_2 = \frac{I(45)-I(135)}{I(45)+I(135)}$, $\eta_3 = \frac{I_+ - I_-}{I_+ + I_-}$ are the Stokes parameters determined by integral intensity values over the cross section of the reflected beam.

Note that the degree of linear polarization and the overall degree of polarization decrease significantly with surface plasmon resonance. When the angle of incidence is outside the SPR region, the polarization state of the reflected beam coincides with the polarization state of the incident beam, and the degree of polarization becomes close to unity (Table 1).

Table 1. Stokes parameters and overall degree of polarization

$\delta\theta = \theta_i - \theta_0$	η_1	η_2	η_3	P_{tot}
0°	0.537	0.028	0.379	0.657
0.1°	0.563	0.308	0.357	0.734
0.5°	0.832	0.477	0.20	0.979

To quantify the spin separation effect, it is advisable to introduce quantitative characteristics such as spin separation purity (SSP) and/or the degree of circular polarization. Degree of circular polarization $P_c = (I_+ - I_-)/(I_+ + I_-)$ of each spot determines the spin-dependent splitting of the

reflected beam. The degree of circular polarization varies depending on the preselection angle and reaches its maximum value at the optimal preselection angle. At a preselection angle of $\gamma = 4^\circ$, the intensity of light with left-handed polarization in the right spot is 20 times higher than the intensity of light with right-handed polarization. This corresponds to a degree of circular polarization exceeding 90%. The spin separation purity can be determined by the parameter $\mu_{\pm} = |I_{\pm}^L - I_{\pm}^R| / (I_{\pm}^L + I_{\pm}^R)$, where the upper indices L and R correspond to the left and right spots, respectively. For the measured powers of $1.32 \mu W$ in the right spot and 65 nW in the left, the spin separation purity $\mu_- > 0.9$.

The degree of separation of circular polarization components (spin separation purity) is almost zero at the preselection angle $\gamma = 0$. This indicates the absence of a spin-dependent shift between the left- and right- circularly polarization components. However, if a non-zero preselection angle is selected, the PSHE can be clearly observed. At the optimal polarization angle of the incident beam (preselection angle), the maximum DOP and the maximum degree of spin separation are achieved. Outside the resonance angle region, the reflected light is predominantly p - polarized.

Usually, the SHE of light is associated with the spatial separation of the field components with left- and right-handed circular polarization. Here, along with the well-known PSHE, we demonstrate a new phenomenon of spatial separation of two orthogonal linearly polarized components corresponding to diagonal polarizations. Note that linear polarization is a coherent superposition of two orthogonal circular polarizations, and circular polarization is a coherent superposition of two orthogonal linear polarizations.

The center of gravity (the x position average) of reflected beams with diagonal polarization is expressed as

$$\langle x_{\pm 45}, \rangle = \frac{\langle E^{\pm 45} | x | E^{\pm 45} \rangle}{\langle E^{\pm 45} | E^{\pm 45} \rangle} = \frac{A}{B+C}, \quad (10)$$

where $E^{\pm 45}$ are the electric fields, which are linearly polarized along the diagonal directions $+45^\circ$ and -45° to the x axis, accordingly, $A = -2|z|\cos^2\gamma[(r_p' \dot{r}_p' + r_p'' \dot{r}_p'')\sin\gamma_1 + (r_p'' \dot{r}_p' - r_p' \dot{r}_p'')\cos\gamma_1] \mp |z|\sin(2\gamma)[(r_s' \dot{r}_p' + r_s'' \dot{r}_p'')\sin\gamma_1 + (r_s'' \dot{r}_p' - r_s' \dot{r}_p'')\cos\gamma_1]$; $B = 2k_0 z_R [|r_p|^2 \cos^2\gamma + |r_s|^2 \sin^2\gamma \pm (r_p' r_s' + r_p'' r_s'')\sin 2\gamma]$; $C = |\dot{r}_p|^2 \cos^2\gamma$; $|z| = \sqrt{z_R^2 + z_f^2}$, $r_{p,s}' = \text{Re}(r_{p,s})$, $r_{p,s}'' = \text{Im}(r_{p,s})$.

In Figure 5, the measured and calculated intensity profiles of reflected beams are presented at a distance $z = 25$ cm from the grating surface. Intensity profiles were obtained after passing linear polarizers at an angle of 45° and 135° relative to the direction of polarization of the incident light. It follows from the results of modeling and experiments that spin-independent separation occurs clearly. This indicates that spatial switching of the reflected beam can be implemented for two orthogonal field components corresponding to diagonal linear polarizations. Unlike PSHE, here linearly polarized photons with zero SAM are spatially separated by optimal preselection and post-selection at weak measurements. Since spinless separation occurs, this effect is not due to spin-orbit coupling. Consequently, angular splitting of circularly polarized photons, as well as linearly polarized photons, occurs near the SPR. As can be seen from Figure 5, the angular shifts are sensitively dependent on both the angle of incidence and the angle of preselection. A particularly high sensitivity is observed with respect to the angle of incidence of the beam (Fig. 5j). When the preselection angle $\gamma = 0^\circ$, there is no spatial separation between the diagonal components.

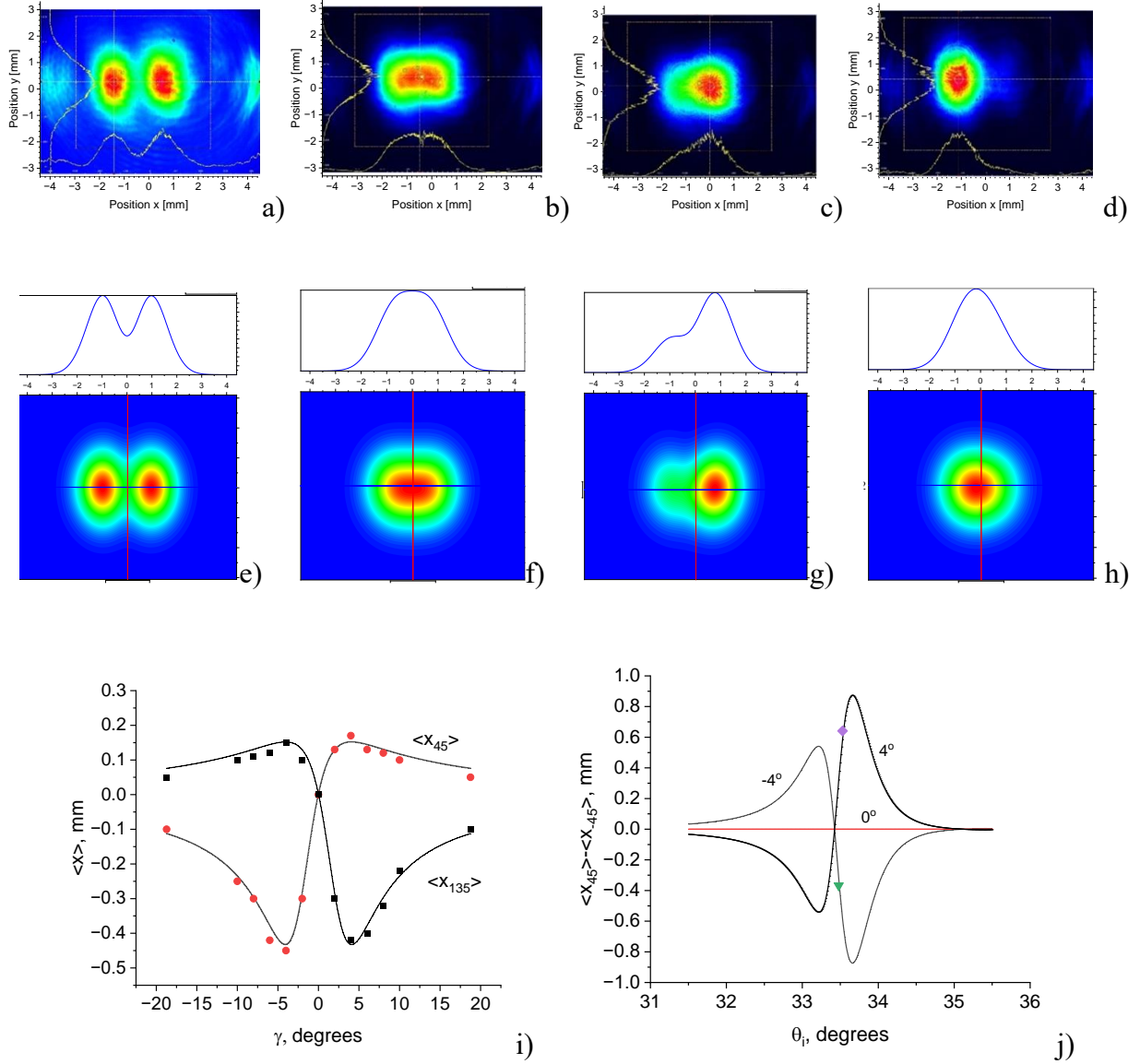


Figure 5. Measured (a-d) and calculated (e-h) intensity profiles of reflected beams at a distance $z = 25$ cm from the grating surface and angle of incidence $\theta_i = 33.53^\circ$. (a, e) $\gamma = 0^\circ$, (b, f) $\gamma = 4^\circ$, (c, g) $I(45^\circ)$, (d, h) $I(135^\circ)$, (i) calculated and measured positions of the centers of gravity depending on the preselection polarization angle, and (j) calculated and measured differences between the centers of gravity of reflected beams polarized at an angle of 45° and 135° degrees depending on angle the incidence.

Physically, the observed effect is due to a change in the phase distribution of the field over the cross section of the reflected beam caused by the interaction of incident radiation with a surface plasmon wave. Indeed, the simulations show that the phases of the reflected fields of p -polarized component at neighboring spots differ by a value of π , i.e., the electric fields fluctuate in opposite phases. The phase of the s -component field remains almost constant over the entire cross section of the reflected beam. Therefore, the left and right spots will be polarized in opposite diagonal directions.

Thus, spin-dependent and spin-independent angular shifts enhanced by SPR have been theoretically and experimentally demonstrated. In contrast to the conventional transverse spin splitting, which is an analogue of the IF shift, here we observed longitudinal spin splitting, which is significantly superior to transverse spin splitting. It is believed that PSHE consists in the separation of photons with opposite spin angular momentum, i.e. in the separation of two orthogonal circular polarizations. Surprisingly, a similar effect can be clearly observed for orthogonally linearly polarized photons. If spin-dependent shifts (spin Hall effect) are the result of spin-orbital interaction, then spin-independent shifts arise because of the phase redistribution of the reflected field at SPR.

Measurements show that the spin splitting increases with a decrease in the size of the focused spot w_0 of the incident beam. We experimentally achieved a spin-dependent angular shift of 13.2 mrad between two reflected spots with opposite spin angular momentum when $w_0 = 17.2 \mu\text{m}$. This displacement corresponds to the spatial separation between the centroids of the reflected spots by 3.1 mm at a distance of 250 mm. These values noticeably exceed the spatial separation of spots with opposite circular polarization observed at the Brewster angle [18-20].

The high sensitivity of SHE to the angle of incidence of the light beam near the surface plasmon resonance has been demonstrated. This indicates that a tunable PSHE can be observed by changing the angle of incidence and a preselected polarization angle near the surface plasmon resonance in subwavelength gratings. The spin separation purity and the degree of circular polarization of each spot reach their maximum value at the optimal preselection angle and the optimal angle of incidence. The polarimetric measurements have shown that the power of the reflected beam at SPR is redistributed into different polarization states. In addition, significant depolarization of light caused by SPR occurs near the resonant incidence angle. Note that although SPR enhances SHE, which is the result of spin-orbit interaction, at the same time it also leads to the depolarization of light. The fact is that the spin-orbit interaction generates effective birefringence in the medium, which, in turn, is one of the sources of depolarization [29-32].

In summary, we demonstrated an enhanced photonic spin Hall effect in a SPR subwavelength structure using standard SHEL theory and polarimetric and optimized weak measurement methods. It is shown that changing the angles of incidence and the polarization state are effective ways to control spin angular splitting, especially to increase its magnitude or switch the spatial position of the reflected beam. Extremely large angular shifts have been demonstrated for a nickel subwavelength grating. We found that these large displacements are very sensitive to the angle of incidence and the state of polarization. Polarimetric measurements demonstrate the depolarization of light caused by SPR and the mixing of polarization states. A high degree of spin separation and a degree of circular polarization are achieved with the optimal polarization state and the resonant incidence angle. A new phenomenon of spinless splitting of two orthogonal field components corresponding to diagonal linear polarizations is demonstrated.

The results obtained can be useful in precision measurement and sensing [33], spectroscopy [34], spin-selective nanophotonic systems [35], in the development of nanophotonic devices, such as beam splitters and switches, and optical sensors.

Funding: Ministry of Science and Higher Education of the Russian Federation (FFNS-2022-0009).

REFERENCES

- (1) Goos, F.; and Hänchen, H. Ein neuer und fundamentaler Versuch zur totalreflexion. *Ann. der Phys.* **1947**, 436, 333-346.
- (2) Fedorov, F.I. K teorii polnovo otrazeniya. *Dokl. Akad. Nauk SSSR* **1955**, 105, 465–468.
- (3) Imbert, C. Calculation and experimental proof of the transverse shift induced by total internal reflection of a circularly polarized light beam. *Phys. Rev. D* **1972**, 5, 787–796.
- (4) Bliokh, K.Y.; Aiello, A. Goos-Hänchen and Imbert-Fedorov beam shifts: an overview. *J. Opt.* **2013**, 15, 014001.
- (5) Yin, X.; Hesselink, L.; Liu, Z.; Fang, N.; and Zhang, X. Large positive and negative lateral optical beam displacements due to surface plasmon resonance. *Appl. Phys. Lett.* **2004**, 85, 372-374.
- (6) Petrov, N.I.; Danilov, V.A.; Popov, V.V.; Usievich, B.A. Large positive and negative Goos-Hänchen shifts near the surface plasmon resonance in subwavelength grating. *Opt. Express* **2020**, 28(5), 7552-7564.
- (7) Petrov, N.I.; Sokolov, Y.M.; Stoiakin, V.V.; Danilov, V.A.; Popov, V.V.; Usievich, B.A. Observation of Giant Angular Goos-Hanchen Shifts Enhanced by Surface Plasmon Resonance in Subwavelength Grating. *Photonics* **2023**, 10, 180.

- (8) Makarova, A.V.; Nerovnaya, A.A.; Gulkin, D.N.; Popov, V.V.; Frolov, A.Yu.; and Fedyanin, A.A. Goos–Hänchen Shift Spatially Resolves Magneto-Optical Kerr Effect Enhancement in Magnetoplasmonic Crystals. *ACS Photonics* **2024**, 11, 1619-1626.
- (9) Soboleva, I.V.; Moskalenko, V.V.; Fedyanin, A.A. Giant Goos-Hanchen effect and Fano resonance at photonic crystal surfaces. *Phys. Rev. Lett.* **2012**, 108, 123901.
- (10) Petrov, N.I. Reflection and transmission of strongly focused light beams at a dielectric interface. *J. Mod. Opt.* **2005**, 52(11), 1545-1556.
- (11) Onoda, M.; Murakami, S.; Nagaosa, N. Hall effect of light. *Phys. Rev. Lett.* **2004**, 93(8), 083901.
- (12) Kavokin, A.; Malpuech, G.; Glazov, M. Optical Spin Hall Effect. *Phys. Rev. Lett.* **2005**, 95, 136601.
- (13) Bliokh, K.Y.; Bliokh, Y.P. Conservation of angular momentum, transverse shift, and spin Hall effect in reflection and refraction of an electromagnetic wave packet. *Phys. Rev. Lett.* **2006**, 96(7), 073903.
- (14) Hosten, O.; and Kwiat, P. Observation of the spin Hall effect of light via weak measurements. *Science* **2008**, 319, 787–790.
- (15) Qin, Y.; Li, Y.; He, H.; Gong, Q. Measurement of spin Hall effect of reflected light. *Opt. Lett.* **2009**, 34(17), 2551–2553.
- (16) Luo, H.; Zhou, X.; Shu, W.; Wen, S.; and Fan, D. Enhanced and switchable spin Hall effect of light near the Brewster angle on reflection. *Phys. Rev. A* **2011**, 84, 043806.
- (17) Qin, Y.; Li, Y.; Feng, X.; Xiao, Y.; Yang, H.; Gong, Q. Observation of the in-plane spin separation of light. *Opt. Expr.* **2011**, 19(10), 9636–9645.

- (18) Zhou, H.; Luo, X.; Wen, S. Weak measurements of a large spin angular splitting of light beam on reflection at the Brewster angle. *Opt. Expr.* **2012**, 20(14), 16003–16009.
- (19) Qiu, X.; Zhang, Z.; Xie, L.; Qiu, J.; Gao, F.; Du, J. Incident-polarization-sensitive and large in-plane-photonic-spin-splitting at the Brewster angle. *Opt. Lett.* **2015**, 40, 1018–1021.
- (20) Zhou, X.; Xie, L.; Ling, X.; Cheng, S.; and Zhang, Z. Large in-plane asymmetric spin angular shifts of a light beam near the critical angle. *Opt. Lett.* **2019**, 44(2), 207–210.
- (21) Sheng, L.; Xie, L.; Sun, J.; Li, S.; Wu, Y.; Chen, Y.; Zhou, X. Tunable in-plane and transverse spin angular shifts in layered dielectric structure. *Opt. Expr.* **2019**, 27(22), 32722–32732.
- (22) Bliokh, K.Y.; Samlan, C.T.; Prajapati, C.; Puentes, G.; Viswanathan, N.K.; and Nori, G. Spin-Hall effect and circular birefringence of a uniaxial crystal plate. *Optica* **2016**, 3, 10, 1039-1047.
- (23) Bliokh, K.Y.; Prajapati, C.; Samlan, C.T.; Viswanathan, N.K.; and Nori, F. Spin-Hall effect of light at a tilted polarizer. *Opt. Lett.* **2019**, 44(19) 4781-4784.
- (24) Kim, M.; Lee, D.; Kim, T.H.; Yang, Y.; Park, H.J.; and Rho, J. Observation of Enhanced Optical Spin Hall Effect in a Vertical Hyperbolic Metamaterial. *ACS Photonics* **2019**, 6, 10, 2530–2536.
- (25) Kim, M.; Lee, D.; Ko, B.; and Rho, J. Diffraction-induced enhancement of optical spin Hall effect in a dielectric grating. *APL Photon.* **2020**, 5, 066106.
- (26) Dai, H.; Yuan, L.; Yin, C.; Cao, Z.; and Chen, X. Direct Visualizing the Spin Hall Effect of Light via Ultrahigh-Order Modes, *Phys. Rev. Lett.* **2020**, 124, 053902.

- (27) Qin, Z.; Yue, C.; Lang, Y.; Liu, Q. Enhancement of spin components' shifts of reflected beam via long range surface plasmon resonance. *Opt. Commun.* **2018**, 426, 16–22.
- (28) You, H.; Alturki, A.; Zeng X.; and Zubairy, M.S. Plasmonic spin induced Imbert–Fedorov shift. *Nanophotonics* **2023**, 12(6), 1159–1167.
- (29) Petrov, N.I., Depolarization of Light in Optical Fibers: Effects of Diffraction and Spin-Orbit Interaction. *Fibers* **2021**, 9, 34.
- (30) Petrov, N.I. Depolarization of Vector Light Beams on Propagation in Free Space. *Photonics* **2022**, 9, 162.
- (31) Petrov, N.I. Evolution of Berry's phase in a graded-index medium. *Phys. Lett. A* **1997**, 234, 239-250.
- (32) Petrov, N.I. Spin-orbit and tensor interactions of light in inhomogeneous isotropic media. *Phys. Rev. A* **2013**, 88, 023815.
- (33) Neugebauer, M.; Nechayev, S.; Vorndran, M.; Leuchs, G.; and Banzer, P. Weak Measurement Enhanced Spin Hall Effect of Light for Particle Displacement Sensing. *Nano Lett.* 2019, 19, 1, 422–425.
- (34) Ni, J.; Liu, S.; Chen, Y.; Hu, G.; Hu, Y.; Chen, W.; Li, J.; Chu, J.; Qiu, C.W.; and Wu, D. Direct Observation of Spin–Orbit Interaction of Light via Chiroptical Responses. *Nano Lett.* **2022**, 22, 9013-9019.
- (35) Thomaschewski, M.; Prämassing, M.; Schill, H.J.; Zenin, V.A.; Bozhevolnyi, S.I.; and Sorger, V.J. Near-Field Observation of the Photonic Spin Hall Effect. *Nano Lett.* **2023**, 23, 24, 11447–11452.